

# Optimal Pre-dilatation Treatment before Implantation of a Magmaris Bioresorbable Scaffold in Coronary Artery Stenosis. The OPTIMIS trial

Kirstine Nørregaard Hansen MD<sup>1,2</sup>, Jens Trøan MD<sup>1</sup>, Akiko Maehara MD<sup>3</sup>, Manijeh Noori MD<sup>1,2</sup>,  
Mikkel Hougaard MD PhD<sup>1</sup>, Julia Ellert-Gregersen MD PhD<sup>1</sup>, Karsten Tange Veien MD<sup>1</sup>, Anders  
Junker MD PhD<sup>1</sup>, Henrik Steen Hansen MD<sup>1,2</sup>, Jens Flensted Lassen MD PhD<sup>1,2</sup>, Lisette Okkels  
Jensen MD DMSci PhD<sup>1,2</sup>

<sup>1</sup>Department of Cardiology, Odense University Hospital, Odense, Denmark

<sup>2</sup>University of Southern Denmark, Odense, Denmark

<sup>3</sup>Cardiovascular Research Foundation, New York Presbyterian Hospital, New York, USA

Short title: Bioresorbable scaffolds and lesion preparation

Word count: 4,805

## *Correspondence to:*

Kirstine Nørregaard Hansen MD  
Odense University Hospital  
Department of Cardiology  
Sdr. Boulevard 29  
5000 Odense C  
Denmark  
E-mail: [kirstinenoerregaard@live.dk](mailto:kirstinenoerregaard@live.dk)  
Phone: +45 6541 2690

NOTE: This preprint reports new research that has not been certified by peer review and should not be used to guide clinical practice.

20 **Abstract**

21 **Introduction:** Bioresorbable scaffolds (BRS) have been developed to overcome limitations related  
22 to late stent failures of drug-eluting-stents, but previous studies have observed lumen reduction over  
23 time after implantation of BRS. The aim of the study was to investigate if lesion preparation with a  
24 scoring balloon compared to a standard non-compliant balloon minimizes lumen reduction after  
25 implantation of a Magmaris BRS (MgBRS) assessed with optical coherence tomography (OCT) and  
26 intravascular ultrasound (IVUS).

27 **Method:** Eighty-two patients with stable angina pectoris were included and randomized in a ratio  
28 1:1 to lesion preparation with either a scoring balloon or a standard non-compliant balloon prior to  
29 implantation of a MgBRS. The primary endpoint was minimal lumen area (MLA) 6 months after  
30 MgBRS implantation.

31 **Results:** Following MgBRS implantation, MLA ( $6.4 \pm 1.6 \text{ mm}^2$  vs.  $6.3 \pm 1.5 \text{ mm}^2$ ,  $p=0.65$ ), mean  
32 scaffold area ( $7.8 \pm 1.5 \text{ mm}^2$  vs.  $7.5 \pm 1.7 \text{ mm}^2$ ,  $p=0.37$ ), and mean lumen area ( $8.0 \pm 1.6 \text{ mm}^2$  vs.  
33  $7.7 \pm 2.1 \text{ mm}^2$ ,  $p=0.41$ ) did not differ significantly in patients where the lesions were prepared with  
34 scoring vs. standard non-compliant balloon respectively. Six-month angiographic follow-up with  
35 OCT and IVUS was available in seventy-four patients. The primary endpoint, 6-months MLA, was  
36 significantly larger in lesions prepared with a scoring balloon compared to a standard non-  
37 compliant balloon ( $4.7 \pm 1.4 \text{ mm}^2$  vs.  $3.9 \pm 1.9 \text{ mm}^2$ ,  $p=0.04$ ), whereas mean lumen area ( $7.2 \pm 1.4$   
38  $\text{mm}^3$  vs.  $6.8 \pm 2.2$ ,  $p=0.35$ ) did not differ significantly. IVUS findings showed no difference in  
39 mean vessel area at the lesion site from baseline to follow-up in the scoring balloon group ( $16.8 \pm$   
40  $2.9 \text{ mm}^2$  vs.  $17.0 \pm 3.6 \text{ mm}^2$ ,  $p=0.62$ ), whereas mean vessel area ( $17.1 \pm 4.4 \text{ mm}^2$  vs.  $15.7 \pm 4.9$   
41  $\text{mm}^2$ ,  $p<0.001$ ) was smaller in lesions prepared with a standard non-compliant balloon due to  
42 negative remodeling.

43 **Conclusion:** Lesion preparation with a scoring balloon prior to implantation of a MgBRS resulted  
44 in significantly larger MLA after 6 months due to less negative remodeling compared to lesion  
45 preparation with a standard non-compliant balloon.

46 Registration: URL: <https://www.clinicaltrials.gov>; Unique identifier: NCT04666584.

47

48 **Clinical perspectives:**

49 What is new?

- 50 - Intense lesion preparation with a scoring balloon prior to implantation of a magnesium-  
51 based Magmaris bioresorbable scaffold results in less lumen reduction and malapposition  
52 after 6 month compared to conventional lesion preparation with a non-compliant balloon in  
53 patients with stable angina.
- 54 - Negative remodeling was seen in lesions treated with conventional lesion preparation,  
55 whereas optimal lesion preparation with a scoring balloon caused in stable remodeling.

56

57 What are the Clinical Implications?

- 58 - Lesions preparation with a scoring balloon is safe and ensures better vascular healing and  
59 vessel dynamics after implantation of a magnesium-based Magmaris bioresorbable scaffold.
- 60 - Optimal lesion preparation should be considered before implantation of magnesium-based  
61 Magmaris bioresorbable scaffold.

<b>Non-standard Abbreviations and Acronyms</b>	
BRS	Bioresorbable scaffold
DAPT	Dual antiplatelet therapy
DES	Drug-eluting stents
EEM	External elastic membrane
IVUS	Intravascular ultrasound
MLA	Minimal lumen area
MgBRS	Magnesium-based Magmaris bioresorbable scaffold
NOAC	Novel oral anticoagulant
OCT	Optical coherence tomography
OPTIMIS	Optimal Pre-dilatation Treatment before Implantation of a Magmaris bioresorbable scaffold In coronary artery Stenosis
PCI	Percutaneous coronary intervention

63 **Introduction**

64 Bioresorbable scaffolds (BRS) were developed to provide temporary vessel support during the early  
65 phases of coronary vessel healing, leaving the artery stent-free after degradation as an alternative to  
66 drug-eluting stents (DES) during percutaneous coronary intervention (PCI)<sup>1,2</sup>. The potential  
67 advantages of BRS were restored vasomotion and potential reduction in late stent failures. The  
68 Absorb everolimus-eluting BRS (Abbott Vascular, Abbott Park, IL, USA) showed increased risk of  
69 scaffold thrombosis and vessel shrinkage over time<sup>3</sup> with significant minimal lumen area (MLA)  
70 reduction after 6 months assessed with optical coherence tomography (OCT)<sup>4</sup>. It is hypothesized  
71 that the mechanism behind lumen reduction is based on decreased radial strength in BRS compared  
72 with bare-metal stents and risk of recoil and scaffold dismantling<sup>5</sup>. The construction of BRS  
73 continued to develop, and different types are now available on the market. The magnesium-based  
74 BRS (Magmaris, Biotronik, Bülach, Switzerland) (MgBRS) was later introduced with improved  
75 radial strength, stronger backbone, change in drug-polymer coating and showed better efficacy  
76 compared to the first BRSs<sup>6-9</sup>. Head-to-head comparison between newer generation DES and the  
77 MgBRS is limited, but the anti-restenotic efficacy has not yet solved the scaffold failure<sup>5,10</sup>.  
78 Optimal lesion preparation prior to implantation of a MgBRS appeared to facilitate optimal scaffold  
79 sizing and better expansion post-procedure in complex lesions<sup>11</sup>, but the effect of aggressive pre-  
80 dilation on vessel and lumen changes over time is uncertain. Peri-procedural intravascular imaging  
81 is recommended during implantation of a MgBRS due to lack of a radiolucent backbone. OCT is  
82 ideal to assess lumen contours<sup>12</sup>, whereas intravascular ultrasound (IVUS) provides information on  
83 the vessel wall and vessel remodeling over time<sup>13,14</sup>. The aim of this study was to assess whether a  
84 more aggressive lesion preparation with a scoring balloon compared to a standard non-compliant  
85 balloon prior to implantation of a MgBRS resulted in less lumen reduction MLA after 6 months.

86

87 **Methods**

88 *Study design*

89 The OPTIMIS (Optimal pre-dilatation Treatment before Implantation of a Magmaris bioresorbable  
90 scaffold In coronary artery Stenosis) study was a prospective, randomized-controlled trial  
91 conducted at Odense University Hospital in Denmark from December 2020 to September 2023. The  
92 study compared lesion preparation with a scoring balloon to a standard non-compliant balloon, prior  
93 to implantation of a MgBRS and the effect on lumen dimension in the scaffold treated segment after  
94 6 months. The patients were randomized to the two pre-dilatation methods in a ratio 1:1. The  
95 primary hypothesis of the OPTIMIS-study was that intense lesion preparation with a scoring  
96 balloon prior to implantation for a MgBRS would result in a larger MLA after 6-month follow-up,  
97 compared to standard pre-dilatation with a non-compliant balloon. A detailed description of the  
98 study design has previously been published<sup>15</sup>.

99 The study was approved by the Regional Committees on Health Research Ethics for Southern  
100 Denmark (Project-ID: S-20200114) and Danish Data Agency (Journal no.: 20/49900), the trial was  
101 registered at ClinicalTrials.gov (NCT04666584).

102

103 *Patient population*

104 Eighty-two patients with stable angina pectoris referred to PCI were enrolled in the study, if they  
105 met the inclusion criteria. Patients were eligible if; 1) age was between 18 and 80 years, 2) if they  
106 had stable angina pectoris, 3) the target lesion was in a native coronary artery, 4) vessel was suitable  
107 for treatment with MgBRS complying with the scaffolds recommended limitations of coronary  
108 artery diameter between  $\geq 2.75$  mm and  $\leq 4.0$  mm measured with OCT or IVUS. Exclusion criteria  
109 were 1) patients participating in other randomized stent studies, 2) expected survival  $< 1$  year, 3)  
110 allergy to aspirin, ticagrelor, clopidogrel or prasugrel, 4) allergy to sirolimus, 4) ostial lesions  
111 (cannot be cleared with flush by OCT), 5) serum creatinine  $> 150$   $\mu\text{g/L}$  (due to the required amount

112 of contrast by OCT), 6) vastly calcified (evaluated with OCT defined as an arc  $> 180^\circ$ , calcium  
113 thickness  $> 0.5$  mm and calcium length of  $> 5$  mm), 7) tortuous coronary arteries where the PCI-  
114 operator estimated that the introduction of an OCT-catheter would not be possible or would be  
115 associated with increased risk, and/or, 8) lesion length  $> 40$  mm. All patients were screened for  
116 protocol inclusion and exclusion criteria before enrolment. Patients underwent clinical and invasive  
117 imaging follow-up with OCT and IVUS at 6 months.

118

### 119 *Antithrombotic therapy*

120 Patients were treated with aspirin 75 mg /day prior to the PCI procedure. On the day for the PCI,  
121 they received a loading dose of 600 mg clopidogrel. Patients were prescribed dual antiplatelet  
122 therapy (DAPT) with aspirin 75 mg /day and clopidogrel 75 mg/day for 6 months followed by  
123 lifelong monotherapy with 75 mg of aspirin. Patients in Warfarin or novel oral anticoagulant  
124 (NOAC) were loaded with 600 mg of clopidogrel. If patients had been admitted and treated for an  
125 acute myocardial infraction within the last 12 months, patients kept their previously prescript  
126 antithrombotic medication.

127

### 128 *Devices*

129 The metallic-based MgBRS contains a magnesium alloy with a bioresobable poly-L-lactide acid  
130 polymer coated with sirolimus as eluting drug released completely after 100 days. The strut  
131 thickness is 150  $\mu\text{m}$ . The MgBRS is completely absorbed after 1 year<sup>16</sup>. The scaffold sizes were  
132 available in a diameter of 3.0 mm and 3.5 mm, and lengths of 15, 20, and 25 mm.

133 The scoring balloon (ScoreFlex, OrbusNeich) catheter is a short mono-rail type balloon catheter. It  
134 provides forced dilatation with a dual-wire semi-compliant balloon system which facilitates local,  
135 safe and controlled plaque modification at lower resolution pressure.



136

137 *Procedure strategy*

138 The coronary stenosis was identified by the PCI operator's interpretation of the angiography and  
139 was treated with a MgBRS in all patients. Patients received a dose of heparin (70 UI/kg) prior to the  
140 procedure. At the discretion of the operator, pre-dilatation with a 2.0 mm balloon was allowed. Pre-  
141 interventional imaging with OCT and IVUS was performed. The scaffold sizing was based on the  
142 external elastic membrane (EEM) diameters of the proximal and distal reference segments. If the  
143 EEM was visible in  $>180^\circ$  of the cross sectional area, the smaller EEM diameter rounded down to  
144 the nearest 0.5 mm was used to determine scaffold diameter. If the EEM was visible in  $<180^\circ$ , the  
145 scaffold diameter was based on the lumen diameter<sup>17</sup>. Patients were allocated 1:1 to either lesion  
146 preparation with 1) a scoring balloon, or 2) a standard non-compliant balloon. The lesion was pre-  
147 dilated in a 1:1 balloon:artery ratio. Up-scaling to a 0.5 mm larger balloon was allowed, if the pre-  
148 dilatation goal was not achieved, as long as the balloon type corresponded to the randomization  
149 arm. The pre-dilatation goal was an angiographic residual stenosis of less than 20%. The lesion was  
150 then treated with implantation of a MgBRS, and inflation pressure was maintained for 30 seconds  
151 during implantation. Mandatory post-dilatation was performed with a non-compliant balloon with  
152 the same size or maximally 0.5 mm larger than the implanted scaffold. Lastly, intravascular  
153 imaging with OCT and IVUS of the scaffold treated segment was performed and controlled by the  
154 PCI-operator and an on-site OCT-analyst. Optimization (if any) was performed at the operators'  
155 discretion. Additional intervention was allowed if there was 1) major under-expansion (minimal  
156 scaffold area (MSA)  $< 4.5 \text{ mm}^2$ ), 2) major malapposition (defined as strut  $> 0.3 \text{ mm}$  from the lumen  
157 wall for  $> 3 \text{ mm}$ ), 3) presence of significant edge dissection, or 4) residual stenosis  $< 5 \text{ mm}$  proximal  
158 or distal to the scaffold (causing MLA  $< 4 \text{ mm}^2$ ). Repeated OCT and IVUS of the final result were

159 then performed. Blinding of the patient, PCI-operator or investigator to pre-dilatation technique was  
160 not possible during the index procedure.

161

#### 162 *Intravascular imaging acquisition*

163 OCT and IVUS were performed at baseline and after 6-month of follow-up. The imaging  
164 procedures were preceded by administration of 200 µg of intracoronary nitroglycerin. OCT was  
165 performed with frequency-domain OPTIS OCT system (Illumien OCT system; Abbott Vascular,  
166 Santa Clara, CA, USA) using the Dragonfly™ Imaging catheter. The catheter was positioned 10  
167 mm distally to the lesion or scaffold-treated segment, and the coronary artery was then flushed with  
168 15 ml contrast injection to clear the artery for blood during automated pullback at a rate of 20 mm/s  
169 over a distance of 75 mm. The IVUS system (Boston Scientific, Marlborough, MA, USA) used a  
170 40MHz OptiCross 2.6 Fr catheter placed 10 mm distally to the lesion or scaffold-treated segment.  
171 Motorized IVUS pullbacks were performed with a pullback speed of 0.5 mm/sec after intracoronary  
172 bolus of 200 µg nitroglycerine.

173

#### 174 *Intravascular imaging analysis*

175 The intravascular imaging pullbacks were analyzed by two independent analysts who were both  
176 blinded to the pre-dilatation technique during analysis. The baseline IVUS and OCT pullbacks were  
177 matched with the follow-up images using anatomical landmarks. OCT offline software (Offline  
178 Review Workstation; Abbott Vascular) was used for quantitative OCT analysis, and the  
179 commercially available program for computerized IVUS-analysis Echoplaque (INDEC Systems,  
180 Inc., Santa Clara, CA, USA) was used for IVUS-analysis. The scaffold-treated segment was  
181 analyzed for every mm. Lumen dimensions at baseline and follow-up were measured: MLA, mean  
182 lumen area, lumen volume, and difference in MLA (follow-up MLA – baseline MLA). Quantitative

183 analysis of scaffold was done using IVUS, because IVUS showed better detection of scaffold  
184 remnants than OCT. Scaffold dimensions at baseline were measured: MSA, mean scaffold area,  
185 minimum scaffold diameter, and scaffold volume. Scaffold malapposition was defined to be present  
186 when the distance between the abluminal surface of the strut and the luminal surface of the vessel  
187 wall exceeded the struts thickness of 150  $\mu\text{m}$ . Major malapposition was defined as struts  $> 0.3$  mm  
188 from the lumen wall for  $>3$  mm in length<sup>18</sup>, and the remaining were classified as minor. At baseline,  
189 malapposition area, distance, and volume were analyzed. At follow-up, visible struts or strut  
190 remnants were categorized as malapposed when the abluminal border of the strut/remnant was  
191 separated from the lumen surface by a visible space exceeding 150  $\mu\text{m}$ . The malapposition  
192 observations was matched from baseline to follow-up and divided into resolved, persistent, or late  
193 acquired malapposition. If a scaffold contained both resolved and persistent malapposition at  
194 follow-up, it was summarized as persistent. To evaluate the effect of pre-dilatation method on  
195 remodeling in the specific lesion site, IVUS was used to identify the pre-procedure MLA in lesion.  
196 The lesion site was defined as 5 mm proximally and distally to MLA. The corresponding 10 mm  
197 segment was identified in IVUS pullback post-procedure and at 6-month follow-up using  
198 anatomical landmarks such as side branches, calcified plaques and scaffold edges. Remodeling was  
199 defined as changes in mean EEM area in the lesion site and deemed significant if the mean EEM  
200 area changed more than  $0.5 \text{ mm}^2$ . Enlargement was defined as positive remodeling, and reduction in  
201 mean EEM area was defined as negative remodeling. Quantitative IVUS analysis included  
202 measurements of EEM, peri-scaffold plaque (EEM area – scaffold area), and total plaque area  
203 (EEM area – lumen area).

204

205 **Statistical analysis**

206 Categorical data was presented as numbers and frequencies and compared using chi-square test or  
207 Fisher's exact statistics. Continuous data was presented as mean  $\pm$  SD and compared using  
208 Student's t-test. Paired t-test was used for comparison from baseline to follow-up. If the distribution  
209 were skewed, a non-parametric test was performed, and median with interquartile range (IQR) was  
210 stated.

211 All tests were two-tailed, and a p-value  $<0.05$  was considered statistically significant. STATA  
212 version 18.0 (StataCorp, Collage Station, TX, USA) was used for the statistical analysis. Inter-  
213 observer variability for imaging analysis was tested for consistency of agreement using an intraclass  
214 correlation coefficient (ICC) was calculated for MLA at follow-up and for malapposition area at  
215 baseline and follow-up. The Pearson correlation coefficient was used to evaluate the direction and  
216 strength of the linear relation between two parameters.

217 The estimated sample size was based on data from the HONEST study<sup>19</sup>. The reduction of MLA  
218 from 6.99 mm<sup>2</sup> to 5.01 mm<sup>2</sup> (27%) 6 months after implantation of the Magmaris BVS, represented  
219 the expected reference group. Optimal lesion preparation with pre-dilatation with a scoring balloon  
220 is estimated to minimize MLA reduction from 6.99 mm<sup>2</sup> to 6.22 mm<sup>2</sup> (11%). A power calculation is  
221 conducted using the expected MLA after 6 months (6.22 mm<sup>2</sup> for the scoring balloon and 5.01 mm<sup>2</sup>  
222 for the standard non-compliant balloon). Inclusion of 35 patients in each group is necessary to reach  
223 statistical significance in case of 2-tailed significance level of 0.05 and power of 80 %. Loss to  
224 follow-up and poor image quality finalize an expected drop-out rate of 15 %, thereby requiring 82  
225 patients in total.

226

## 227 **Endpoints**

228 The primary endpoint was MLA in the scaffold-treated segment pre-dilated with a scoring balloon  
229 versus standard non-compliant balloon 6-month after implantation of a MgBRS assessed with OCT.

230 Secondary endpoints were differences between treatment groups in: 1) change in MLA, and 2)  
231 percentage and size of incomplete scaffold apposition at baseline and follow-up.

232

## 233 **Results**

234 A flowchart of enrolled patients is provided in Figure 1.

235 In total, 82 patients were enrolled in the study. Follow-up images were not available in 8 patients  
236 due to following reasons. One patient randomized to standard non-compliant balloon pre-dilatation  
237 was excluded due to vessel dissection that could not be covered by a MgBRS scaffold. Two patients  
238 were excluded, one in the scoring balloon group and one in the standard non-compliant balloon  
239 group, due to scaffold failure where the MgBRS was lost in the coronary artery proximally to the  
240 study lesion. In all three cases, patients were treated with a DES. Five patients had unavailable  
241 follow-up images: Two patients withdrew consents (one in the scoring balloon group and one  
242 standard non-compliant balloon group), one patient died within the 6-month angiographic follow-up  
243 (standard non-compliant balloon group), one patient had a subacute scaffold thrombosis 5 days after  
244 implantation (standard non-compliant balloon group), and one patient was postponed due to nurses'  
245 strike (standard non-compliant balloon group).

246

### 247 *Clinical and procedural characteristics*

248 Baseline clinical and procedural characteristics are presented in Table 1 and Table 2.

249 The treatment groups were well matched without any significant differences in baseline  
250 characteristics. Also, there were no significant differences in procedural characteristics, except for  
251 balloon length which was significantly shorter in the scoring balloon group (only available in 10  
252 and 15 mm) ( $13.1 \pm 2.5$  mm vs.  $15.5 \pm 3.3$  mm,  $p < 0.001$ ) compared to the standard non-compliant  
253 balloon group.

254

255 *Optical coherence tomography findings*

256 Post-procedure and 6-month follow-up OCT findings are presented in Table 3. Inter-observer  
257 variability for MLA at follow-up was: ICC=0.996 (95% confidence interval (CI): 0.999-1.00,  
258  $p < 0.001$ ), for total malapposition area at baseline: ICC=0.949 (95% CI: 0.77-0.99,  $p < 0.001$ ), and  
259 for total malapposition at follow-up: ICC=0.874 (95% CI: 0.50-0.97,  $p = 0.001$ ).

260

261 Lumen dimensions

262 At baseline, there was no significant difference in MLA, mean LA, or lumen volume between the  
263 two treatment groups assessed with OCT. At 6-month follow-up, MLA (the primary endpoint) in  
264 the scaffold-treated segment was significantly larger in the patients allocated to pre-dilatation with a  
265 scoring balloon, compared to a standard non-compliant balloon ( $4.71 \text{ mm}^2 \pm 1.35$  vs.  $3.91 \text{ mm}^2 \pm$   
266  $1.86$ ,  $p = 0.04$ ). There was no significant difference between the two groups in mean LA, or lumen  
267 volume at 6-month follow-up. There was a relative reduction in MLA of -24.8% for the scoring  
268 balloon group compared to -38.3% in the standard non-compliant balloon group,  $p = 0.009$ .  
269 Representative cases of lumen reduction from baseline to follow-up are shown in Figure 2.

270

271 Scaffold measurements and malapposition

272 At baseline, scaffold parameters, such as scaffold length, mean scaffold area, minimal scaffold area,  
273 and total scaffold volume were similar in the two groups. Total number of analyzable struts were  
274 similar at baseline between the two groups ( $199.9 \pm 70.5$  in the scoring balloon group and  $210.7 \pm$   
275  $60.0$  in the standard non-compliant balloon group,  $p = 0.46$ ). At follow-up, the total number of  
276 analyzable struts were reduced to  $70.8 \pm 35.1$  in the scoring balloon group and  $85.1 \pm 32.1$  in the  
277 standard non-compliant balloon group ( $p = 0.07$ ).

278 At baseline, half of the scaffolds in both groups had minor malapposition. There were no major  
279 malappositions in any of the groups. Percentage of malapposed struts was small in both groups and  
280 significantly lower in the scoring balloon group with 1.5 % compared to 4.6 % in the standard non-  
281 compliant balloon group (p=0.02). At baseline, malapposition volume tended to be smaller in the  
282 scoring balloon group (0.38 mm<sup>2</sup> [0.15 ; 0.95]) compared to the standard non-compliant balloon  
283 group [1.07 mm<sup>2</sup> 0.48 ; 2.27], but there was no significant difference (p= 0.09).

284 At 6-month follow-up, 15.4% of the lesions treated with the scoring balloon had minor  
285 malappositions, whereas 42.9% in the standard balloon group had minor malappositions (p=0.009).  
286 There significantly smaller total malapposition volume (0.0 [0.0 ; 0.0] vs. 0.21 [0.0 ; 0.59],  
287 p=0.009) and percentage of malapposed struts (0.0 [0.0 ; 0.0] vs. 1.62 [0.0 ; 3.49], p=0.004) in the  
288 scoring group compared to the standard non-compliant balloon group at 6-month follow-up. Type  
289 of malapposition did not differ between groups. Malappositions were resolved in 31.4 % of the  
290 scaffolds in the scoring balloon group, compared to 48.6% in the standard non-compliant balloon  
291 group. In the scoring balloon group, 5% had persistent malapposition vs. 20% in the standard  
292 balloon group. Late acquired malapposition was seen in 15.4% in the scoring balloon group  
293 compared to 22.9% in the standard non-compliant balloon group, and often positioned at scaffold  
294 edge and in relation to calcified plaque. Malapposition types are presented in Figure 3.

295 At 6-month follow-up, no scaffold area and volume were drawn since most of the struts were  
296 absorbed. OCT images of scaffold degradation are shown in Figure 2. The total number of struts  
297 were similar in the two groups, but there were significantly less struts per cross section in the  
298 scoring balloon group compared to standard non-compliant balloon group after 6 months.

299

300 *Intravascular ultrasound findings*

301 Post-procedure and 6-month follow-up IVUS findings are presented in Table 3 and Table 4 and  
302 Supplementary table 1.

303

#### 304 Vessel dimensions

305 There was no difference in vessel measurements between the two groups at baseline or at 6-month  
306 follow-up (Table 3). The paired analysis of mean area in the 10 mm lesion site and corresponding  
307 segment post-procedure and at 6-month follow-up are presented in Table 4. There was no  
308 significant difference in mean lumen area from post-procedure to 6-month follow-up in the scoring  
309 balloon group ( $8.5 \pm 1.4 \text{ mm}^2$  vs.  $8.1 \pm 1.8 \text{ mm}^2$ ,  $p=0.08$ ), whereas a significant decrease in lumen  
310 area was found in the standard non-compliant balloon group ( $8.2 \pm 1.7 \text{ mm}^2$  vs.  $7.4 \pm 2.6 \text{ mm}^2$ ,  
311  $p=0.009$ ). Vessel area in the 10 mm segment corresponding to the lesion site did not change in the  
312 scoring balloon group from baseline to 6-month follow-up ( $16.8 \pm 2.9 \text{ mm}^2$  vs.  $17.0 \pm 3.6 \text{ mm}^2$ ,  
313  $p=0.62$ ), but was significantly decreased ( $17.1 \pm 4.4 \text{ mm}^2$  vs.  $15.7 \pm 4.9 \text{ mm}^2$ ,  $p < 0.001$ ) in the  
314 standard non-compliant balloon group indicating negative remodeling.

315

#### 316 Pattern of remodeling

317 Figure 4 shows the relationship between relative change in lumen area and relative change in vessel  
318 area (A), and relative change in lumen area and relative change in plaque area (B). There was a  
319 significant positive correlation between relative change in lumen area and relative change in vessel  
320 area at the 10 mm lesion site ( $r=0.72$ , 95% CI: 0.58-0.81,  $p<0.001$ ), but there was no correlation  
321 between relative change in lumen area and relative change in plaque area ( $r=-0.02$ , 95% CI: -0.25-  
322 0.21,  $p=0.88$ ).

323



324 *Clinical 6-month follow-up*

325 In patients allocated to pre-dilatation with a scoring balloon prior to implantation of the MgBRS  
326 one patient had a target vessel revascularization not related to the scaffold-treated segment. There  
327 were no events observed corresponding to the scaffold-treated segment in the scoring balloon  
328 group. In patients treated with the standard balloon prior to implantation of the MgBRS following  
329 events were observed: one patient admitted with STEMI and subacute scaffold thrombosis 5 days  
330 after index procedure. This patient was only treated with aspirin for 4 days followed by  
331 monotherapy with clopidogrel as the patient also received NOAC; one patient died due to an  
332 intracranial hemorrhage 92 days after index procedure.

333

334 **Discussion**

335 In summary, we found that MLA assessed with OCT was significantly larger in the scoring balloon  
336 group compared to the standard non-compliant balloon group 6 month after implantation of the  
337 MgBRS. In both groups, MLA decreased from baseline to 6-month follow-up, but less MLA  
338 reduction was seen in the scoring balloon group compared to the standard non-compliant balloon  
339 group. At the lesion site, there was no change in remodeling from baseline to follow-up in the  
340 scoring balloon group, whereas negative remodeling was observed in lesions prepared with the  
341 standard non-compliant balloon. In the lesions pre-dilated with a scoring balloon, there was  
342 significantly less malapposition at follow-up compared to the standard non-compliant balloon  
343 group.

344 The magnesium-based BRS was first evaluated in the DREAM 1G study<sup>20</sup>, where a significant  
345 decrease in MLA was observed within the first 6 months ( $7.9 \text{ mm}^2 \pm 1.2$  vs.  $5.7 \text{ mm}^2 \pm 1.0$ ) after  
346 implantation assessed with OCT. The second generation magnesium-based BRS, MgBRS, had  
347 higher flexibility and higher radial force, than the first generation magnesium-based BRS<sup>21</sup>.

348 Previous studies have investigated the vascular healing after 6 months of the magnesium-based  
349 BRS with both IVUS and OCT, but significant lumen decrease continued to occur<sup>6, 19, 22, 23</sup>.  
350 Assessed with OCT, malapposition, neointimal hyperplasia and strut coverage were near impossible  
351 to detect at follow-up, because the strut remnants had lost their metallic stent-like appearance  
352 during the absorption process. Interestingly, the BIOSOLVE-II study (BIOtroniks – Safety and  
353 performance in de novo Lesion of native coronary arteries with Magmaris) reported measurable  
354 scaffold observation, such as mean and minimum scaffold area and incomplete strut apposition as  
355 visible with IVUS, but not with OCT at 6-month follow-up<sup>22</sup>. The same pattern applied to our  
356 findings, where scaffold area detection was not possible with OCT, but analyzable with IVUS at 6-  
357 month follow-up. The BIOSOLVE-II trial<sup>22</sup> measured smaller lumen and scaffold areas assessed  
358 with IVUS compared to OCT, which was unlike our findings with smaller lumen and scaffold  
359 measurements evaluated with OCT compared to IVUS. IVUS is often reported to overestimate  
360 lumen area compared to OCT<sup>17</sup>, which may explain why no difference was found between the two  
361 groups when using IVUS in lumen or scaffold measurements.

362 A third generation magnesium-based BRS (DREAMS-3G) has been developed with larger size  
363 range, thinner struts (99/117/147  $\mu\text{m}$  vs. 150  $\mu\text{m}$ ), and increased radial strength<sup>24</sup> compared to the  
364 MgBRS used in our study. An absolute reduction in MLA was  $-2.4 \text{ mm}^2$  (from  $7.2 \text{ mm}^2$  to  $4.8 \text{ mm}^2$   
365 at 6-month follow-up) for the DREAMS-3G, which was comparable to our results in the standard  
366 non-compliant balloon group with an absolute reduction of  $-2.3 \text{ mm}^2$ . The scoring balloon group in  
367 our study had less absolute reduction of  $-1.7 \text{ mm}^2$ . Even though, we found a significant difference  
368 in MLA between the two groups, we still revealed lumen reduction in both groups from baseline to  
369 6-month follow-up. Lumen reduction of 25% was considerably larger than the expected 11% lumen  
370 reduction anticipated in our power calculation.

371 The HONEST trial<sup>25</sup> comparing OCT- and angio-guided implantation with the MgBRS in a  
372 population with acute coronary syndrome found a significant reduction in MLA observed after 6  
373 month in both groups with a relative difference of 33.2 % and 22.8 % in MLA, respectively. The  
374 mechanism behind lumen reduction may be due to additional post-dilatation in an attempt to  
375 optimize the apposition, resulting in fracture or dismantling of the scaffold hence reducing the  
376 radial strength<sup>26</sup>. Other mechanisms contributing to premature lumen loss after implantation of the  
377 MgBRS could be scaffold recoil, neointimal hyperplasia and impact of underlying plaque  
378 morphology and vessel remodeling<sup>5</sup>. The pattern of remodeling, with significant correlation  
379 between change in lumen area and change in vessel area, but not between change in lumen area and  
380 plaque area, indicated vessel reduction and not plaque increase as the overall reason for lumen  
381 reduction. The pattern of remodeling was similar in the two groups, but the overall magnitude of  
382 vessel reduction causing lumen reduction was larger in the standard non-compliant balloon group  
383 compared the scoring balloon group. Our results reported significantly more decrease in vessel area  
384 in lesions prepared with a standard non-compliant balloon, which was not seen in the lesions pre-  
385 dilated with the scoring balloon. This indicates that negative remodeling and vessel shrinkage may  
386 be contributing factors for lumen loss in our study in the standard non-compliant balloon group. In  
387 the ABSORB Cohort B trial, dynamics of the vessel wall was investigated with IVUS after  
388 implantation the everolimus-eluting bioresorbable ABSORB scaffold. They reported no evidence of  
389 late recoil, but enlargement of the vessel, lumen and scaffold area up to three years after  
390 implantation<sup>27</sup>. The early resorption of the MgBRS with fast loss of radial force has been suggested  
391 as a limiting factor to the device, and must be investigated further<sup>5</sup>. The extent of scaffold recoil is a  
392 balance between elastic recoil and radial strength and can be affected by the fibrotic plaque in the  
393 coronary artery in the treated segment<sup>5</sup>. Optimal pre-dilatation with a more aggressive lesion  
394 preparation could result in a better vascular healing and less lumen reduction<sup>11</sup>. More lipid-rich

395 plaques have been associated with less lumen loss after implantation of the MgBRS, whereas the  
396 constrictive vascular forces and rigidity of fibrotic plaque may facilitate lumen reduction<sup>5</sup>. Patients  
397 with acute coronary syndrome tend to have lesions with more lipid-rich plaque and positive  
398 remodeling compared to our population of patients with stable coronary syndrome, which could  
399 explain more lumen reduction than expected in the current study.

400 Percentage of post-procedure malapposed struts was small in our study in both groups (1.46% for  
401 scoring balloon group and 4.57% for the standard non-compliant balloon group). As shown in  
402 previous trials<sup>5, 19, 20, 22</sup>, most struts will not be visible after 6 months, due to the fast scaffold  
403 absorption. Even though we found up to 43% of the scaffolds with malapposition had follow-up, the  
404 percentage of malapposed struts and malapposition volume was low. Significantly less  
405 malapposition was present in the scoring balloon group compared to the standard non-compliant  
406 balloon group, which contributes to the assumption of better vascular healing after lesion  
407 preparation with a scoring balloon. To determine if these findings are a part of the natural healing  
408 process needs longer follow-up time.

409 Despite reported lumen loss after implantation of the MgBRS in various intravascular imaging  
410 studies<sup>19, 22</sup>, the clinical performance is still deemed safe and efficient in several studies. Registries  
411 have reported safety and efficacy with low 1-year TLF rates of 3.3-5.4% and stent thrombosis rates  
412 of 0.5%, and TLF of 7.8% and scaffold thrombosis of 0.5% up to 24 months after implantation<sup>9, 28,</sup>  
413 <sup>29</sup>. A registry study found no difference in 24-month clinical outcomes between patients with acute  
414 vs. stable coronary syndromes who were treated with a MgBRS<sup>30</sup>. Only few studies have compared  
415 the MgBRS to DES, for example the MAGSTEMI trial (MAGnesium-based bioresorbable scaffold  
416 in ST-segment Elevation Myocardial Infarction) that showed a significantly higher TLF rate in the  
417 MgBRS group after 1 year in a ST-segment elevation myocardial infarction population<sup>10</sup>. However,  
418 a retrospective cohort reported similar 1-year clinical outcome comparing the MgBRS to a

419 biodegradable polymer DES in a non-ST-segment elevation myocardial infarction cohort<sup>31</sup>. More  
420 randomized controlled trials with long-term follow-up are needed to fully illuminate the clinical  
421 benefits or disadvantages between the new generation BRS and traditional DES.

422

### 423 **Limitations**

424 There are some potential limitations to this study. The study was not powered to correlate clinical  
425 endpoints with OCT and IVUS findings. The study was conducted during the COVID-19 pandemic  
426 and was furthermore challenged by nurse strike and delivery problems of OCT catheters, why the  
427 inclusion period was unexpectedly prolonged. Also, the patient and lesion selections were  
428 influenced by limited available scaffold sizes.

429

### 430 **Conclusion**

431 After 6 months, lesion preparation with a scoring balloon, compared to a standard non-compliant  
432 balloon, prior to implantation of a MgBRS resulted in larger MLA, no remodeling and less  
433 malapposition, whereas negative remodeling was seen in the standard non-compliant balloon group.

434

### 435 **Sources of funding**

436 The study is an investigator-initiated trial, and did not receive any financial support.

437

### 438 **Declaration of competing Interest**

439 KNH, MN, JT, COF, MH, KTV, JEG, AJ, AM, JFL, HSH have no conflict of interests. LOJ has  
440 received research grants from Biotronik, OrbusNeich, Biosensors, and Terumo to her institution.

441

## 442 References

- 443 1. Azzi N, Shatila W. Update on coronary artery bioresorbable vascular scaffolds in percutaneous  
444 coronary revascularization. *Rev Cardiovasc Med.* 2021;22:137-145
- 445 2. Serruys PW, Katagiri Y, Sotomi Y, Zeng Y, Chevalier B, van der Schaaf RJ, et al. Arterial  
446 remodeling after bioresorbable scaffolds and metallic stents. *Journal of the American College of*  
447 *Cardiology.* 2017;70:60-74
- 448 3. Ali ZA, Serruys PW, Kimura T, Gao R, Ellis SG, Kereiakes DJ, et al. 2-year outcomes with the  
449 absorb bioresorbable scaffold for treatment of coronary artery disease: A systematic review and  
450 meta-analysis of seven randomised trials with an individual patient data substudy. *Lancet (London,*  
451 *England).* 2017;390:760-772
- 452 4. Serruys PW, Onuma Y, Ormiston JA, de Bruyne B, Regar E, Dudek D, et al. Evaluation of the  
453 second generation of a bioresorbable everolimus drug-eluting vascular scaffold for treatment of de  
454 novo coronary artery stenosis: Six-month clinical and imaging outcomes. *Circulation.*  
455 2010;122:2301-2312
- 456 5. Ueki Y, Räber L, Otsuka T, Rai H, Losdat S, Windecker S, et al. Mechanism of drug-eluting  
457 absorbable metal scaffold restenosis: A serial optical coherence tomography study. *Circulation.*  
458 *Cardiovascular interventions.* 2020;13:e008657
- 459 6. Haude M, Erbel R, Erne P, Verheye S, Degen H, Böse D, et al. Safety and performance of the drug-  
460 eluting absorbable metal scaffold (dreams) in patients with de-novo coronary lesions: 12 month  
461 results of the prospective, multicentre, first-in-man biosolve-i trial. *Lancet (London, England).*  
462 2013;381:836-844
- 463 7. Haude M, Ince H, Toelg R, Lemos PA, von Birgelen C, Christiansen EH, et al. Safety and  
464 performance of the second-generation drug-eluting absorbable metal scaffold (dreams 2g) in patients  
465 with de novo coronary lesions: Three-year clinical results and angiographic findings of the biosolve-  
466 ii first-in-man trial. *EuroIntervention : journal of EuroPCR in collaboration with the Working Group*  
467 *on Interventional Cardiology of the European Society of Cardiology.* 2020;15:e1375-e1382
- 468 8. Haude M, Toelg R, Lemos PA, Christiansen EH, Abizaid A, von Birgelen C, et al. Sustained safety  
469 and performance of a second-generation sirolimus-eluting absorbable metal scaffold: Long-term data  
470 of the biosolve-ii first-in-man trial at 5 years. *Cardiovascular revascularization medicine : including*  
471 *molecular interventions.* 2022;38:106-110
- 472 9. Verheye S, Wlodarczak A, Montorsi P, Torzewski J, Bennett J, Haude M, et al. Biosolve-iv-registry:  
473 Safety and performance of the magmaris scaffold: 12-month outcomes of the first cohort of 1,075  
474 patients. *Catheterization and cardiovascular interventions : official journal of the Society for*  
475 *Cardiac Angiography & Interventions.* 2021;98:E1-e8
- 476 10. Sabaté M, Alfonso F, Cequier A, Romaní S, Bordes P, Serra A, et al. Magnesium-based resorbable  
477 scaffold versus permanent metallic sirolimus-eluting stent in patients with st-segment elevation  
478 myocardial infarction: The magstemi randomized clinical trial. *Circulation.* 2019;140:1904-1916
- 479 11. Miyazaki T, Latib A, Ruparelia N, Kawamoto H, Sato K, Figini F, et al. The use of a scoring balloon  
480 for optimal lesion preparation prior to bioresorbable scaffold implantation: A comparison with  
481 conventional balloon predilatation. *EuroIntervention : journal of EuroPCR in collaboration with the*  
482 *Working Group on Interventional Cardiology of the European Society of Cardiology.*  
483 2016;11:e1580-1588
- 484 12. Tearney GJ, Regar E, Akasaka T, Adriaenssens T, Barlis P, Bezerra HG, et al. Consensus standards  
485 for acquisition, measurement, and reporting of intravascular optical coherence tomography studies:  
486 A report from the international working group for intravascular optical coherence tomography  
487 standardization and validation. *Journal of the American College of Cardiology.* 2012;59:1058-1072
- 488 13. Mintz GS, Guagliumi G. Intravascular imaging in coronary artery disease. *Lancet (London,*  
489 *England).* 2017;390:793-809
- 490 14. Mintz GS, Nissen SE, Anderson WD, Bailey SR, Erbel R, Fitzgerald PJ, et al. American college of  
491 cardiology clinical expert consensus document on standards for acquisition, measurement and  
492 reporting of intravascular ultrasound studies (ivus). A report of the american college of cardiology

- 493 task force on clinical expert consensus documents. *Journal of the American College of Cardiology*.  
494 2001;37:1478-1492
- 495 15. Hansen KN, Maehara A, Noori M, Trøan J, Fallesen CO, Hougaard M, et al. Optimal lesion  
496 preparation before implantation of a magmaris bioresorbable scaffold in patients with coronary  
497 artery stenosis: Rationale, design and methodology of the optimis study. *Contemp Clin Trials*  
498 *Commun*. 2024;38:101260
- 499 16. Gutiérrez-Chico JL, Cortés C, Schincariol M, Limon U, Yalcinli M, Durán-Cortés MA, et al.  
500 Implantation of bioresorbable scaffolds under guidance of optical coherence tomography: Feasibility  
501 and pilot clinical results of a systematic protocol. *Cardiology journal*. 2018;25:443-458
- 502 17. Maehara A, Matsumura M, Ali ZA, Mintz GS, Stone GW. Ivus-guided versus oct-guided  
503 coronary stent implantation: A critical appraisal. *JACC. Cardiovascular imaging*. 2017;10:1487-  
504 1503
- 505 18. Shlofmitz E, Croce K, Bezerra H, Sheth T, Chehab B, West NEJ, et al. The mld max oct algorithm:  
506 An imaging-based workflow for percutaneous coronary intervention. *Catheterization and*  
507 *Cardiovascular Interventions*. 2022;100:S7-S13
- 508 19. Fallesen CO, Antonsen L, Maehara A, Noori M, Hougaard M, Hansen KN, et al. Optical coherence  
509 tomography- versus angiography-guided magnesium bioresorbable scaffold implantation in nstemi  
510 patients. *Cardiovascular revascularization medicine : including molecular interventions*.  
511 2022;40:101-110
- 512 20. Waksman R, Prati F, Bruining N, Haude M, Böse D, Kitabata H, et al. Serial observation of drug-  
513 eluting absorbable metal scaffold: Multi-imaging modality assessment. *Circulation. Cardiovascular*  
514 *interventions*. 2013;6:644-653
- 515 21. Waksman R, Zumstein P, Pritsch M, Wittchow E, Haude M, Lapointe-Corriveau C, et al. Second-  
516 generation magnesium scaffold magmaris: Device design and preclinical evaluation in a porcine  
517 coronary artery model. *EuroIntervention : journal of EuroPCR in collaboration with the Working*  
518 *Group on Interventional Cardiology of the European Society of Cardiology*. 2017;13:440-449
- 519 22. Haude M, Ince H, Abizaid A, Toelg R, Lemos PA, von Birgelen C, et al. Safety and performance of  
520 the second-generation drug-eluting absorbable metal scaffold in patients with de-novo coronary  
521 artery lesions (biosolve-ii): 6 month results of a prospective, multicentre, non-randomised, first-in-  
522 man trial. *Lancet (London, England)*. 2016;387:31-39
- 523 23. Tovar Forero MN, van Zandvoort L, Masdjedi K, Diletti R, Wilschut J, de Jaegere PP, et al. Serial  
524 invasive imaging follow-up of the first clinical experience with the magmaris magnesium  
525 bioresorbable scaffold. *Catheterization and cardiovascular interventions : official journal of the*  
526 *Society for Cardiac Angiography & Interventions*. 2020;95:226-231
- 527 24. Haude M, Wlodarczak A, van der Schaaf RJ, Torzewski J, Ferdinande B, Escaned J, et al. Safety and  
528 performance of the third-generation drug-eluting resorbable coronary magnesium scaffold system in  
529 the treatment of subjects with de novo coronary artery lesions: 6-month results of the prospective,  
530 multicenter biomag-i first-in-human study. *EClinicalMedicine*. 2023;59:101940
- 531 25. Fallesen CO, Maehara A, Antonsen L, Nørregaard Hansen K, Noori M, Flensted Lassen J, et al.  
532 Coronary artery healing process after bioresorbable scaffold in patients with non-st-segment  
533 elevation myocardial infarction: Rationale, design, and methodology of the honest study.  
534 *Cardiology*. 2021:1-11
- 535 26. Barkholt T, Webber B, Holm NR, Ormiston JA. Mechanical properties of the drug-eluting  
536 bioresorbable magnesium scaffold compared with polymeric scaffolds and a permanent metallic  
537 drug-eluting stent. *Catheterization and cardiovascular interventions : official journal of the Society*  
538 *for Cardiac Angiography & Interventions*. 2020;96:E674-e682
- 539 27. Serruys PW, Onuma Y, Garcia-Garcia HM, Muramatsu T, van Geuns RJ, de Bruyne B, et al.  
540 Dynamics of vessel wall changes following the implantation of the absorb everolimus-eluting  
541 bioresorbable vascular scaffold: A multi-imaging modality study at 6, 12, 24 and 36 months.  
542 *EuroIntervention : journal of EuroPCR in collaboration with the Working Group on Interventional*  
543 *Cardiology of the European Society of Cardiology*. 2014;9:1271-1284
- 544 28. Galli S, Troiano S, Pallosi A, Rapetto C, Pisano F, Aprigliano G, et al. Sustained safety and  
545 efficacy of magnesium reabsorbable scaffold: 2-year follow-up analysis from first magmaris

- 546 multicenter italian registry. *Cardiovascular revascularization medicine : including molecular*  
547 *interventions*. 2022;41:69-75
- 548 29. Haude M, Ince H, Kische S, Abizaid A, Tölg R, Alves Lemos P, et al. Safety and clinical  
549 performance of a drug eluting absorbable metal scaffold in the treatment of subjects with de novo  
550 lesions in native coronary arteries: Pooled 12-month outcomes of biosolve-ii and biosolve-iii.  
551 *Catheterization and cardiovascular interventions : official journal of the Society for Cardiac*  
552 *Angiography & Interventions*. 2018;92:E502-e511
- 553 30. Galli S, Troiano S, Palloshi A, Rapetto C, Pisano F, Aprigliano G, et al. Comparison of acute versus  
554 stable coronary syndrome in patients treated with the magmaris scaffold: Two-year results from the  
555 magmaris multicenter italian registry. *Cardiovascular revascularization medicine : including*  
556 *molecular interventions*. 2023;57:53-59
- 557 31. Rola P, Włodarczak A, Włodarczak S, Barycki M, Szudrowicz M, Łanocha M, et al. Magnesium  
558 bioresorbable scaffold (brs) magmaris vs biodegradable polymer des ultimaster in nste-acs  
559 population-12-month clinical outcome. *Journal of interventional cardiology*. 2022;2022:5223317
- 560



<b>Table 1: Patient baseline characteristics</b>		
	<b>Scoring balloon</b>	<b>Standard balloon</b>
	<b>N = 41</b>	<b>N = 41</b>
Age, years	64.9 ± 9.0	64.8 ± 7.9
Male, n (%)	27 (65.9)	28 (68.3)
Family history of IHD, n (%)	19 (46.3)	17 (41.5)
History of smoking, n (%)		
Current smoker	6 (14.6)	6 (14.6)
Previous smoker	21 (51.2)	11 (26.8)
Hypertension, n (%)	17 (41.5)	25 (61.0)
Hypercholesterolemia, n (%)	11 (26.8)	13 (31.7)
Diabetes mellitus, n (%)	4 (9.8)	8 (19.5)
Body mass index, kg/m <sup>2</sup>	27.9 ± 9.7	27.9 ± 3.7
eGFR, ml/min	79.7 ± 12.5	82.1 ± 11.6
Previous myocardial infarction, n (%)	9 (22.0)	4 (9.8)
Previous PCI, n (%)	11 (26.8)	6 (14.6)
Previous CABG, n (%)	0 (0.0)	0 (0.0)
CABG = coronary bypass graft, eGFR = estimated glomerular filtration rate, IHD = ischemic heart disease, PCI = percutaneous coronary intervention. Data is shown as mean ± standard deviation.		

561

562

<b>Table 2: Procedural and angiographic characteristics</b>		
	Scoring balloon	Standard balloon
	N = 41	N = 41
Target coronary artery, n (%)		
Left anterior descending	23 (56.1)	24 (58.5)
Left circumflex	6 (14.6)	8 (19.5)
Right coronary artery	12 (29.3)	9 (22.0)
Lesion length, mm	23.9 ± 10.5	22.5 ± 5.4
Reference vessel diameter, mm	3.4 ± 0.3	3.4 ± 0.3
Pre-dilatation, n (%)	41 (100)	41 (100)
Balloon diameter at pre-dilatation, mm	3.3 ± 0.3	3.3 ± 0.3
Balloon length at pre-dilatation, mm	13.1 ± 2.5*	15.5 ± 3.3
Max balloon pressure at pre-dilatation, atm	13.1 ± 2.8	14.0 ± 2.7
Number of scaffolds per lesion, mm	1.1 ± 0.3	1.1 ± 0.2
Scaffold length, mm	19.4 ± 4.1	21.0 ± 3.9
Scaffold diameter, mm	3.3 ± 0.2	3.3 ± 0.3
Maximum balloon pressure, atm	11.9 ± 2.2	12.0 ± 2.4
Expected scaffold diameter, mm	3.4 ± 0.3	3.4 ± 0.3
Post-dilatation, n (%)	38 (93)	41 (100)
Balloon diameter at post-dilatation, mm	3.7 ± 0.3	3.7 ± 0.4
Balloon length at post-dilatation, mm	14.5 ± 3.6	15.7 ± 3.3
Max balloon pressure at post-dilatation, atm	13.0 ± 2.6	12.8 ± 2.4
Flouro time, minutes	12.3 ± 5.3	11.8 ± 5.2

Contrast volume, ml	108.0 ± 42.9	102.6 ± 43.8
Procedure time, minutes	49.9 ± 17.7	47.9 ± 18.4
* significantly shorter balloon length at pre-dilatation in the scoring balloon group (p-value < 0.001)		

<b>Table 3: Post-procedure and 6-month follow-up optical coherence tomography findings and intravascular ultrasound</b>						
	Baseline			6-month follow-up		
	Scoring balloon	Standard balloon	p-value	Scoring balloon	Standard balloon	p-value
<b>OCT finding</b>						
Number of patients	40	38		39	35	
Time to 6-month follow-up, days				185 [182 ; 234]	184 [182 ; 192]	0.29
Lumen measurement						
Minimal lumen area, mm <sup>2</sup>	6.42 ± 1.55	6.27 ± 1.48	0.65	4.71 ± 1.35	3.91 ± 1.86	0.04
Difference in minimal lumen area (6 months - baseline), mm <sup>2</sup>				-1.70 ± 1.49	-2.30 ± 1.42	0.08
Relative change in minimal lumen area (6 months - baseline), %				-24.8 ± 20.4	-38.3 ± 22.7	0.009
Mean lumen area, mm <sup>2</sup>	8.01 ± 1.62	7.66 ± 2.12	0.41	7.21 ± 1.41	6.79 ± 2.21	0.35
Total lumen volume, mm <sup>3</sup>	167.31 ± 50.82	169.47 ± 54.70	0.86	151.50 ± 53.94	139.93 ± 52.95	0.36
Difference in total lumen volume (6 months - baseline), mm <sup>3</sup>				-16.99 ± 21.35	-25.35 ± 28.45	0.16
Relative change in total lumen volume (6 months - baseline), %				-10.5 ± 11.7	-15.0 ± 16.8	0.20

Scaffold measurement						
Total number of analyzable struts	199.9 ± 70.5	210.7 ± 60.0	0.46	70.8 ± 35.1	85.1 ± 32.1	0.07
Mean no. of struts per cross section	9.11 ± 0.71	9.11 ± 0.82	1.00	3.1 ± 1.3	3.9 ± 1.7	0.03
Scaffold length, mm	20.8 [16.5 ; 24.1]	22.2 [19.2 ; 24.8]	0.51	20.4 [17.2 ; 24.0]	21.0 [17.2 ; 25.2]	0.69
Minimal scaffold area, mm <sup>2</sup>	6.40 ± 1.50	6.09 ± 1.51	0.36			
Mean scaffold area, mm <sup>2</sup>	7.77 ± 1.49	7.45 ± 1.69	0.37			
Total scaffold volume, mm <sup>3</sup>	161.81 ± 45.93	160.88 ± 52.44	0.93			
Scaffold malapposition						
Scaffold malapposition, n (%)	20 (50.0)	21 (55.3)	0.64	6 (15.4)	15 (42.9)	0.009
Total malapposition volume, mm <sup>3</sup>	0.38 [0.15 ; 0.95]	1.07 [0.48 ; 2.27]	0.09	0.0 [0.0 ; 0.0]	0.21 [0.0 ; 0.59]	0.009
Mean malapposition distance, mm	0.23 [0.21 ; 0.28]	0.30 [0.25 ; 0.34]	0.003	0.0 [0.0 ; 0.0]	0.18 [0.0 ; 0.4]	0.004
Percentage of malapposed struts, %	1.5 [0.6 ; 3.0]	4.57 [1.7 ; 5.8]	0.02	0.0 [0.0 ; 0.0]	1.6 [0.0 ; 3.5]	0.004
Types of incomplete stent apposition						
Resolved, n (%)				17 (48.6)	11 (31.4)	0.28
Persistent, n (%)				2 (5.0)	7 (20.0)	0.05
Late acquired, n (%)				4 (10.3)	8 (22.9)	0.14

<b>Intravascular ultrasound</b>						
Number of patients	40	38		39	34	
Time to 6-month follow-up, days				183 [153 ; 290]	183.5 [134 ; 225]	0.66
Vessel measurements						
EEM area at MLA site, mm <sup>2</sup>	14.73 ± 3.39	16.19 ± 4.87	0.13	13.53 ± 3.50	13.70 ± 4.69	0.86
Mean EEM area, mm <sup>2</sup>	16.70 ± 2.87	16.96 ± 4.22	0.75	16.24 ± 3.23	15.59 ± 4.66	0.50
Total EEM volume, mm <sup>3</sup>	361.61 ± 97.49	383.88 ± 130.23	0.40	353.91 ± 120.67	336.85 ± 110.95	0.53

563

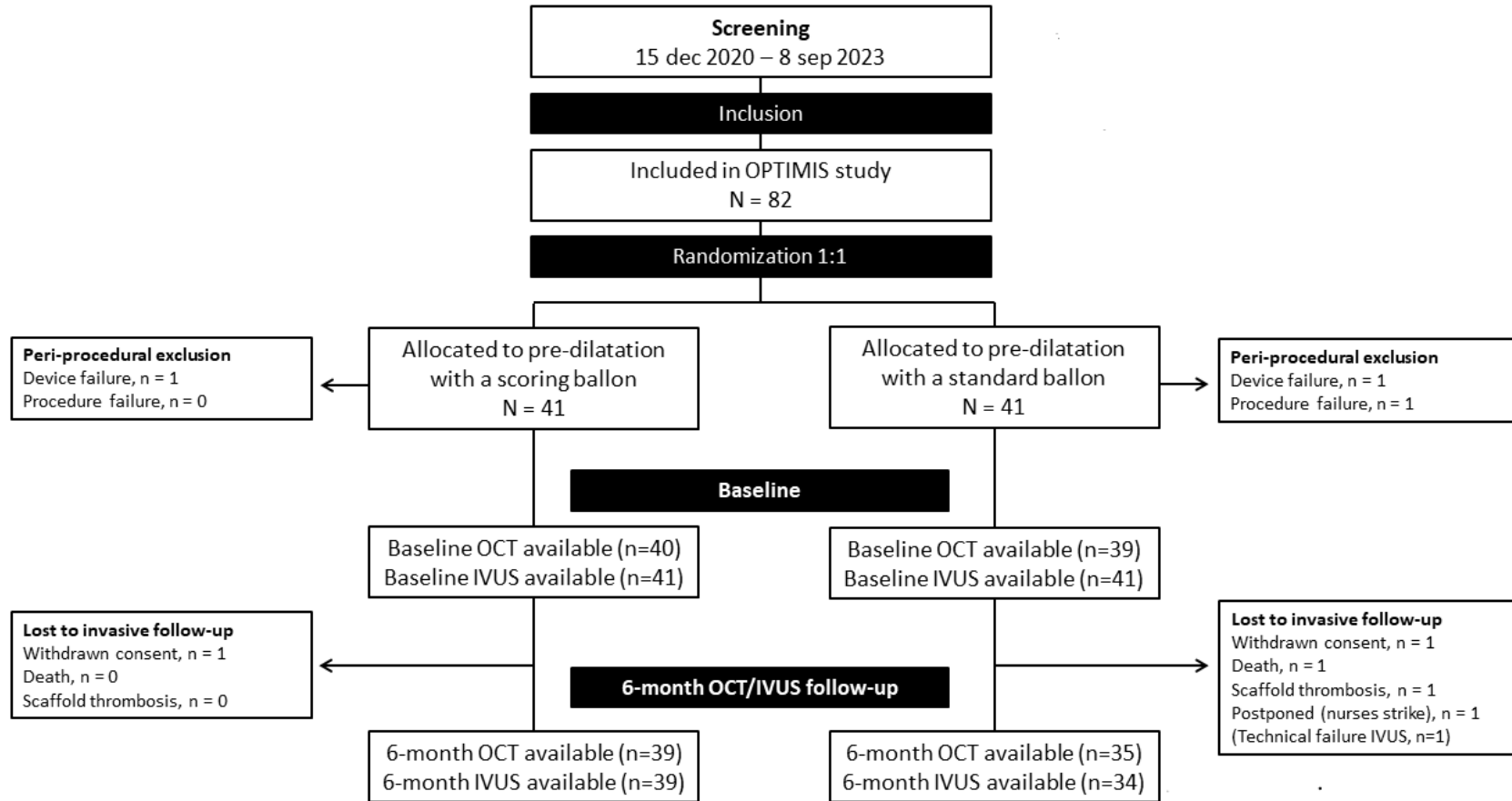
564

<b>Table 4: Remodeling of lesion segment pre-procedure and corresponding segment post-procedure and at 6-month follow-up assessed with IVUS</b>			
	Scoring N = 39	Standard N = 34	p-value
<b>Mean lumen (mm<sup>2</sup>)</b>			
Pre-procedure	5.3 ± 1.4	4.8 ± 1.5	0.13
Post-procedure	8.5 ± 1.4	8.2 ± 1.7	0.31
6-month follow-up	8.1 ± 1.8	7.4 ± 2.6	0.19
Change (6 months – baseline)	-0.4 ± 1.5	-0.8 ± 1.6	0.41
p-value (baseline vs. 6 months)*	0.08	0.009	
<b>Mean EEM area (mm<sup>2</sup>)</b>			
Pre-procedure	13.3 ± 3.1	13.4 ± 4.8	0.88
Post-procedure	16.8 ± 2.9	17.1 ± 4.4	0.74
6-month follow-up	17.0 ± 3.6	15.7 ± 4.9	0.20
Change (6 months – baseline)	0.2 ± 2.0	-1.4 ± 2.0	0.001
p-value (baseline vs. 6 months)*	0.62	< 0.001	
<b>Mean plaque area (mm<sup>2</sup>)</b>			
Pre-procedure	7.9 ± 2.5	8.6 ± 3.9	0.39
Post-procedure	8.3 ± 2.0	8.9 ± 3.5	0.31
6-month follow-up	8.9 ± 2.4	8.3 ± 3.0	0.36
Change (6 months – baseline)	0.6 ± 1.3	-0.7 ± 1.9	0.002
p-value (baseline vs. 6 months)*	0.007	0.06	
<b>Mean scaffold area (mm<sup>2</sup>)</b>			

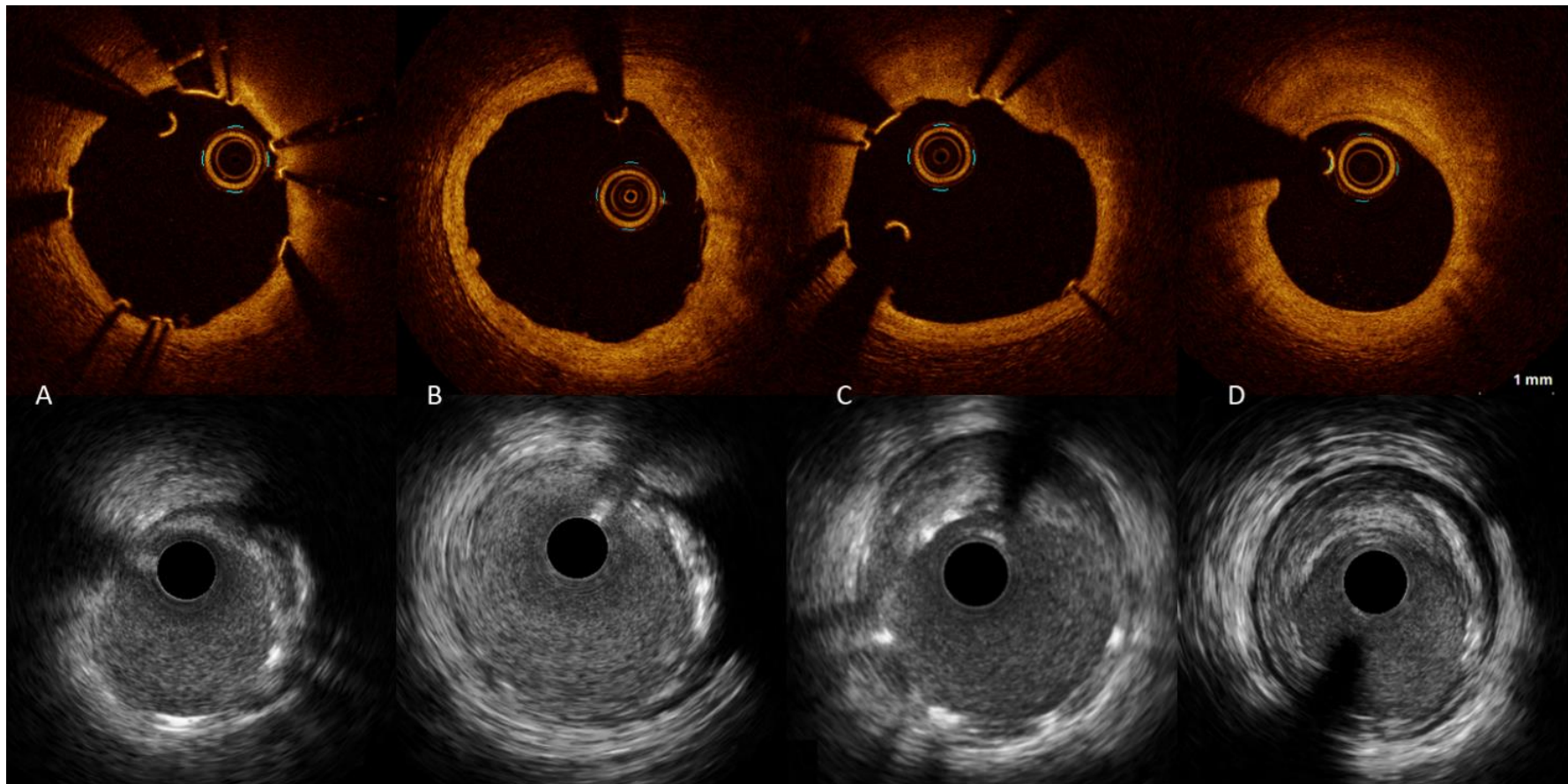
Post-procedure	$9.5 \pm 1.7$	$9.1 \pm 1.9$	0.26
6-month follow-up	$10.1 \pm 2.1$	$8.9 \pm 2.8$	0.04
Change (6 months – baseline)	$0.6 \pm 1.9$	$-0.2 \pm 1.8$	0.10
p-value (baseline vs. 6 months)*	0.07	0.58	
*paired analysis			



566 Figure 1: Flow chart



568 Figure 2: Intravascular images of lumen reduction after implantation of Magmaris bioresorbable scaffold.

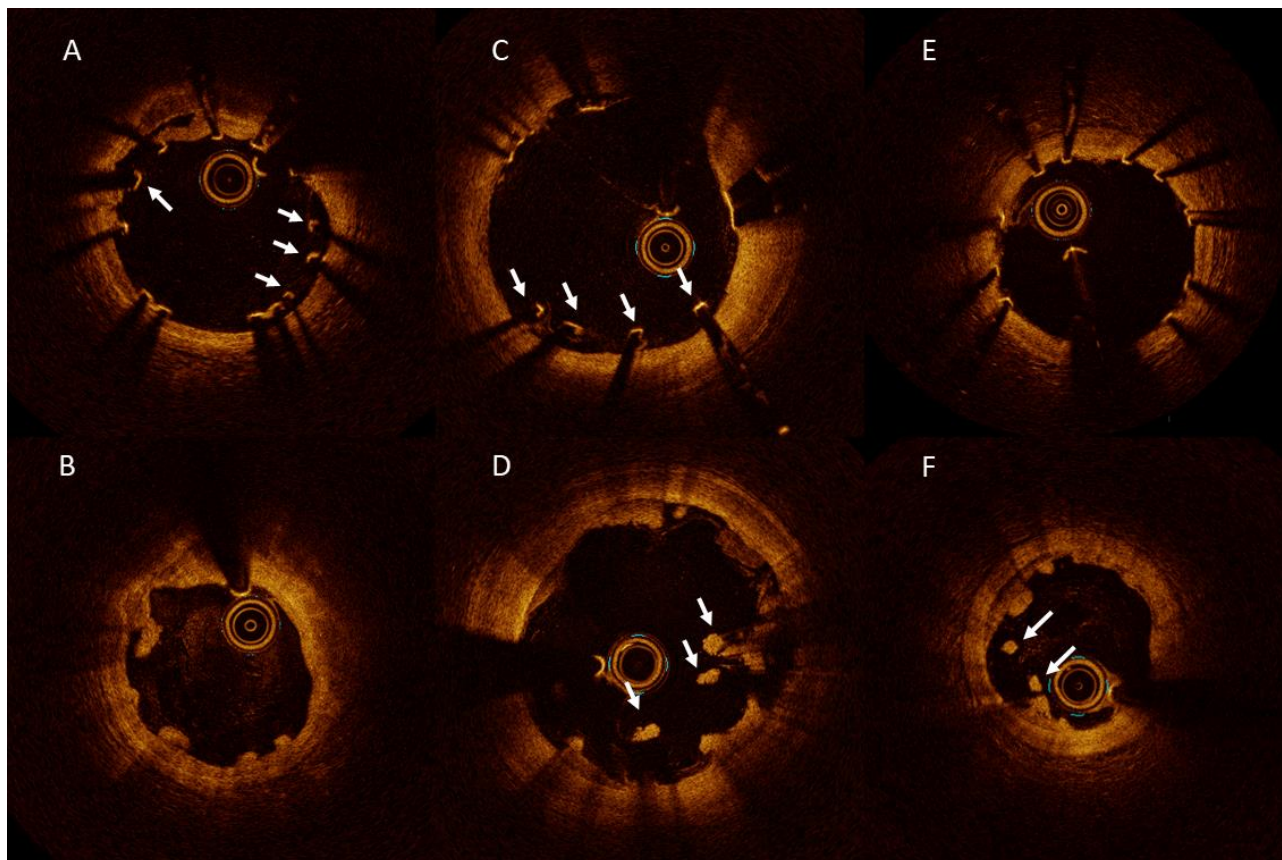


569  
 570 The upper panel shows OCT images of minimal lumen area from baseline and the corresponding site at follow-up. The lower panel shows  
 571 the matching site acquired with IVUS. Images A and B represent the vascular healing after lesion preparation with a scoring balloon prior  
 572 to MgBRS implantation. Lumen area at baseline was  $7.3 \text{ mm}^2$  measured with OCT and  $7.5 \text{ mm}^2$  with IVUS. Vessel area was  $12.7 \text{ mm}^2$  at

573 baseline (A). At 6-month follow-up, lumen area was 8.8 mm<sup>2</sup> with OCT and 8.8 mm<sup>2</sup> with IVUS. Vessel area was 16.0 mm<sup>2</sup> (B). Images C  
574 and D represent the vascular healing after implantation of a MgBRS in a lesion pre-dilated with a standard non-compliant balloon. Lumen  
575 area at baseline was 8.8 mm<sup>2</sup> with OCT and 8.8 mm<sup>2</sup> with IVUS. Vessel area was 16.0 mm<sup>2</sup> (C). After 6 months, the matching site was  
576 reduced to 5.1 mm<sup>2</sup> measured with OCT, and 5.6 mm<sup>2</sup> with IVUS. Vessel area was 13.8 mm<sup>2</sup> (D). Abbreviations: IVUS = Intravascular  
577 ultrasound; MgBRS = Magmaris bioresorbable scaffold; OCT = Optical coherence tomography.

578

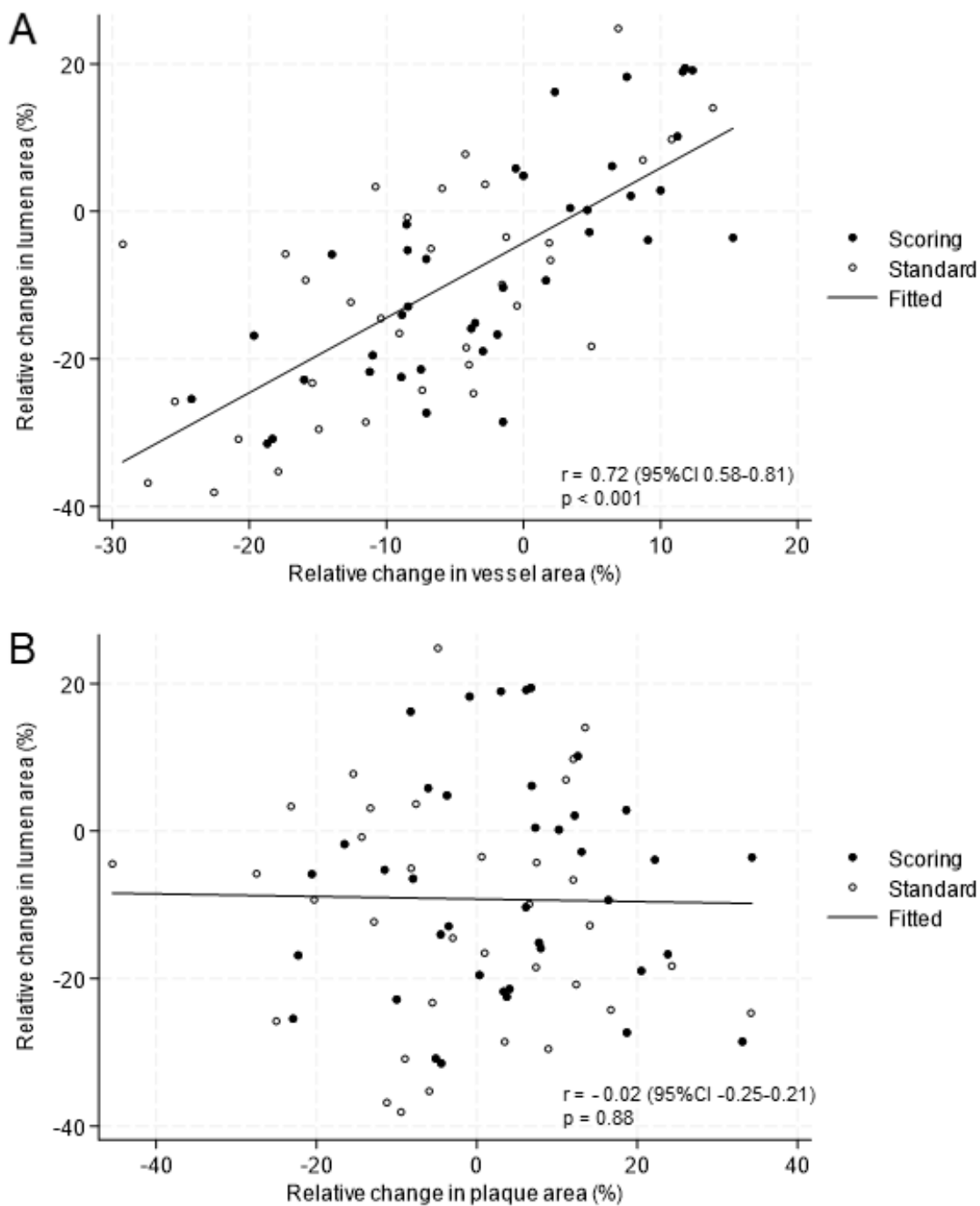
579 Figure 3: Optical coherence tomography images of malapposition types



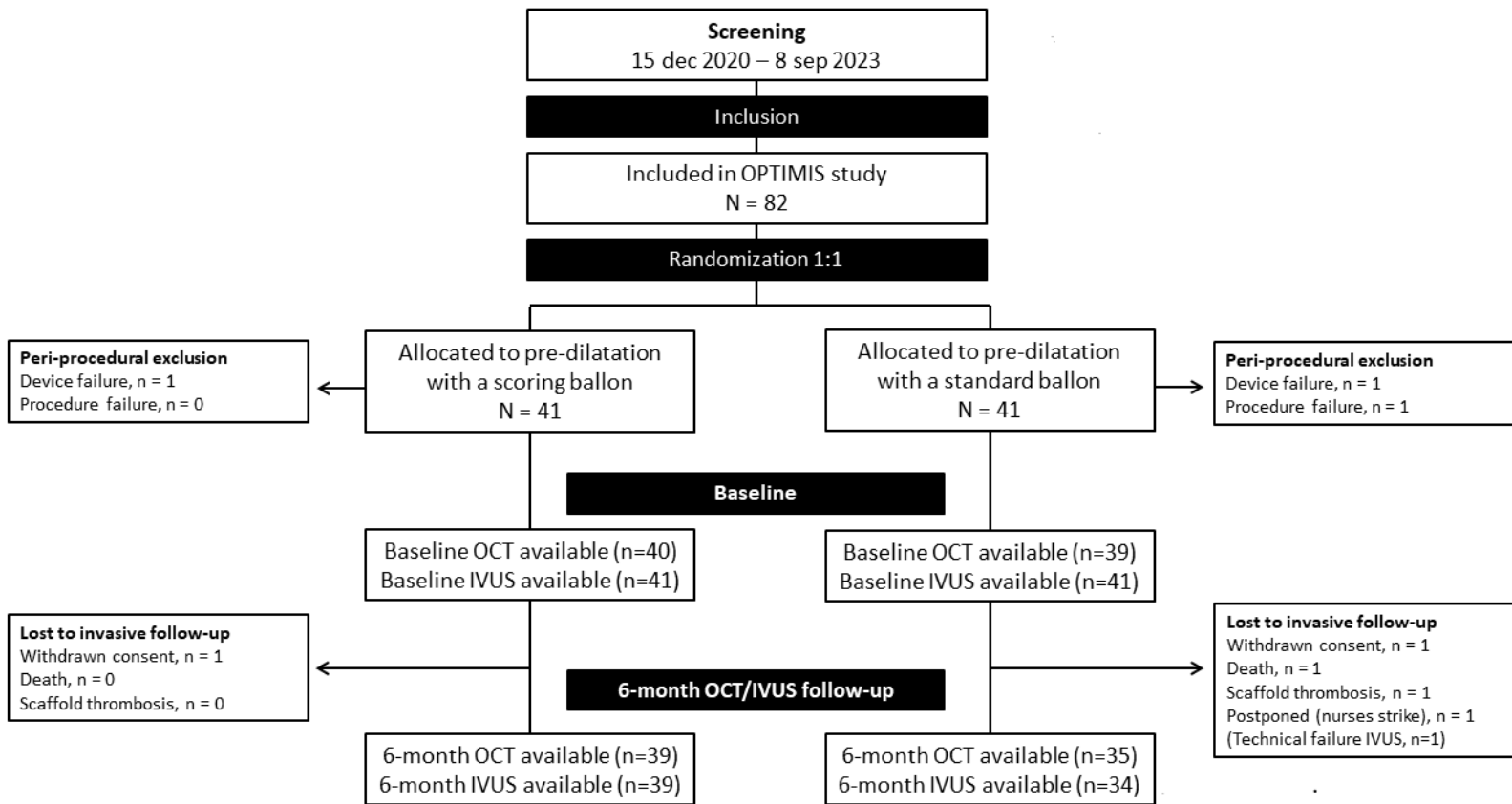
580

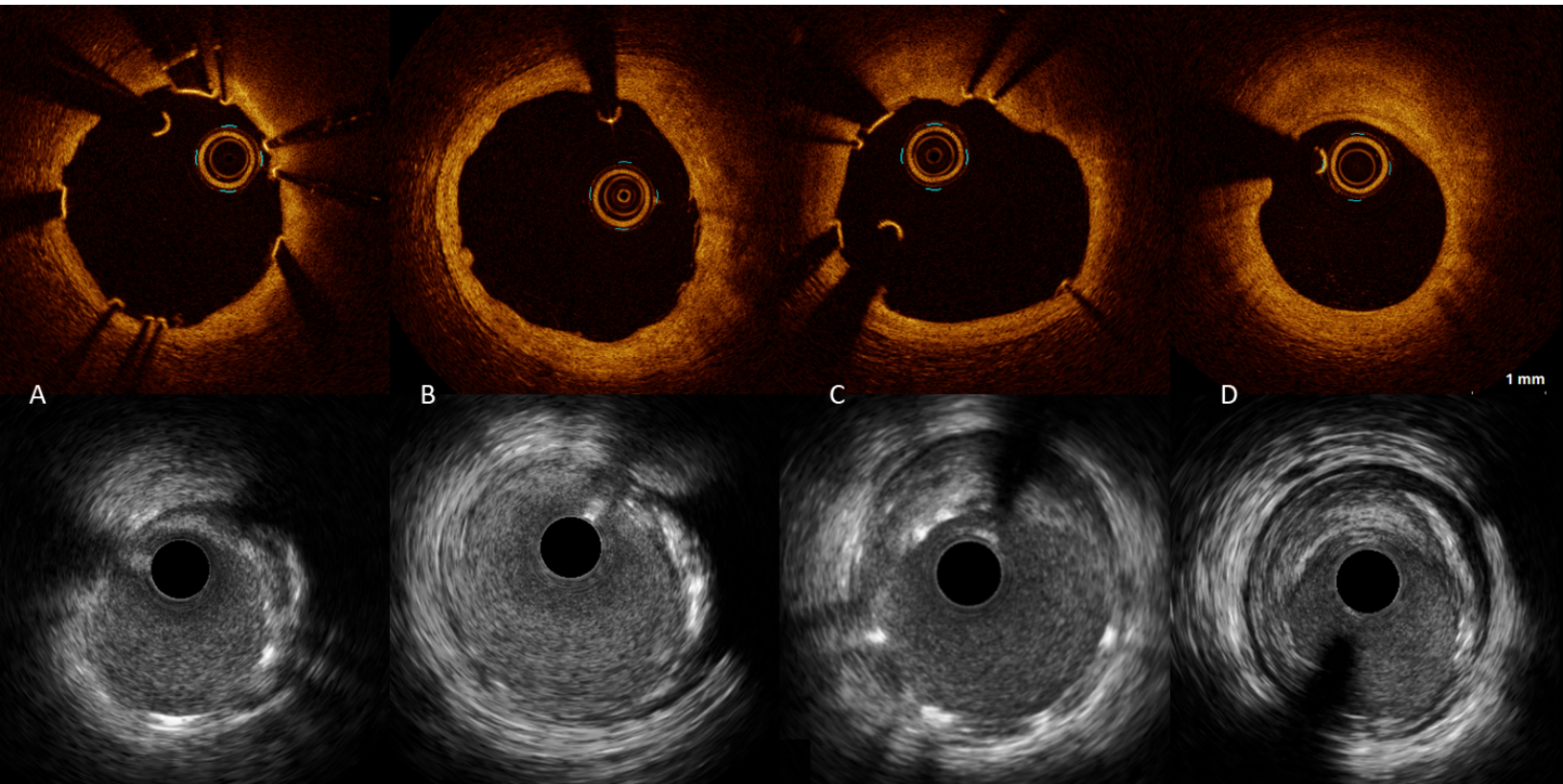
581 Upper panel represents baseline optical coherence tomography images, and lower panel represents  
582 6-month follow-up. A) There are three malapposed struts from 3 to 5 o'clock, and one malapposed  
583 strut at 10 o'clock. The corresponding site after 6 months (B) revealed resolved malapposition from  
584 3 to 5 o'clock, but persistent malapposition at 10 o'clock. C) Four malapposed struts are visible at  
585 baseline from 5 to 7 o'clock. At 6-month follow-up, persistent malapposition is seen in the  
586 corresponding cross section (D). E) All struts are well-apposed, but after 6 month acquired  
587 malapposition appears at 7 to 8 o'clock.

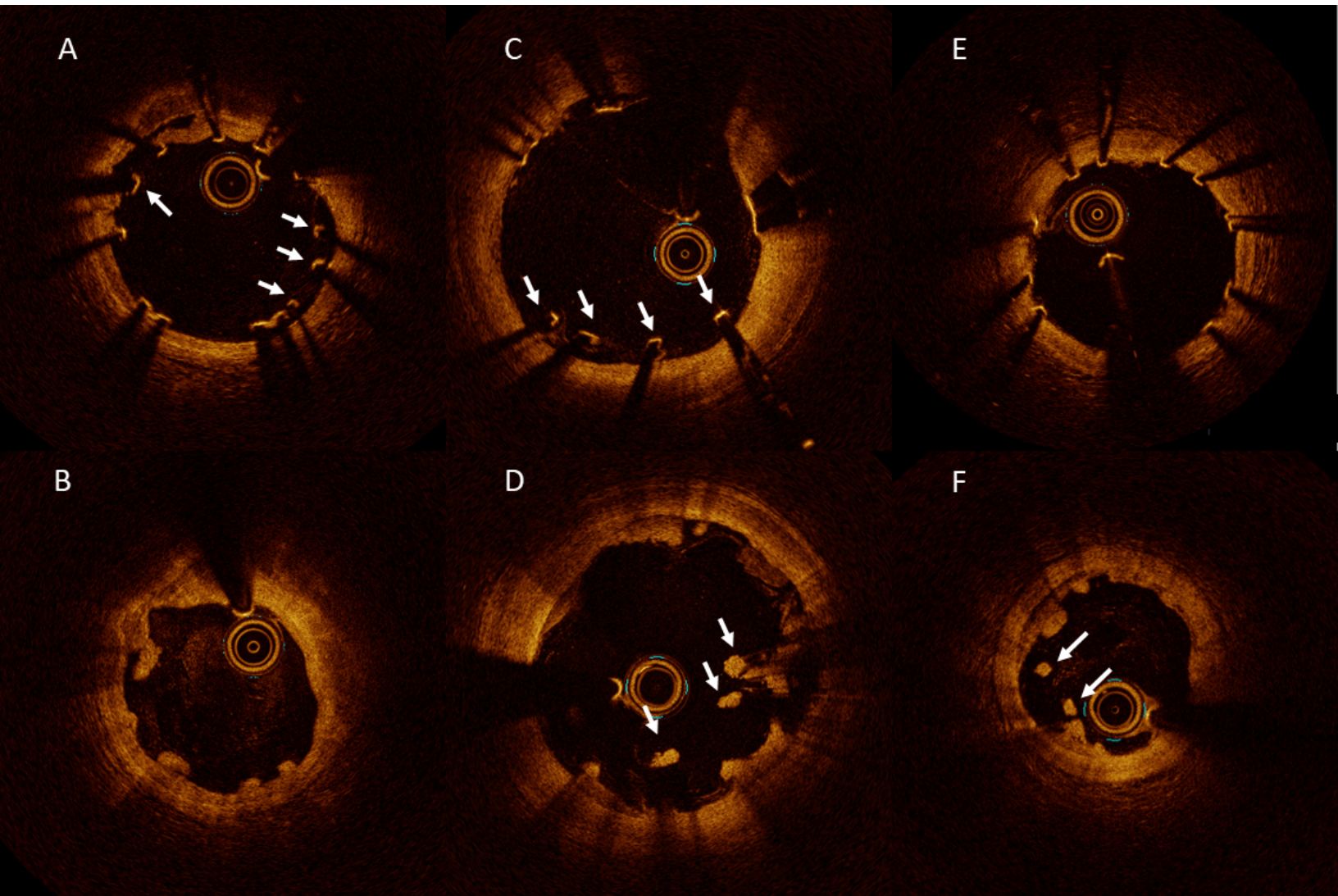
Figure 4: Pattern of remodeling at the lesion site



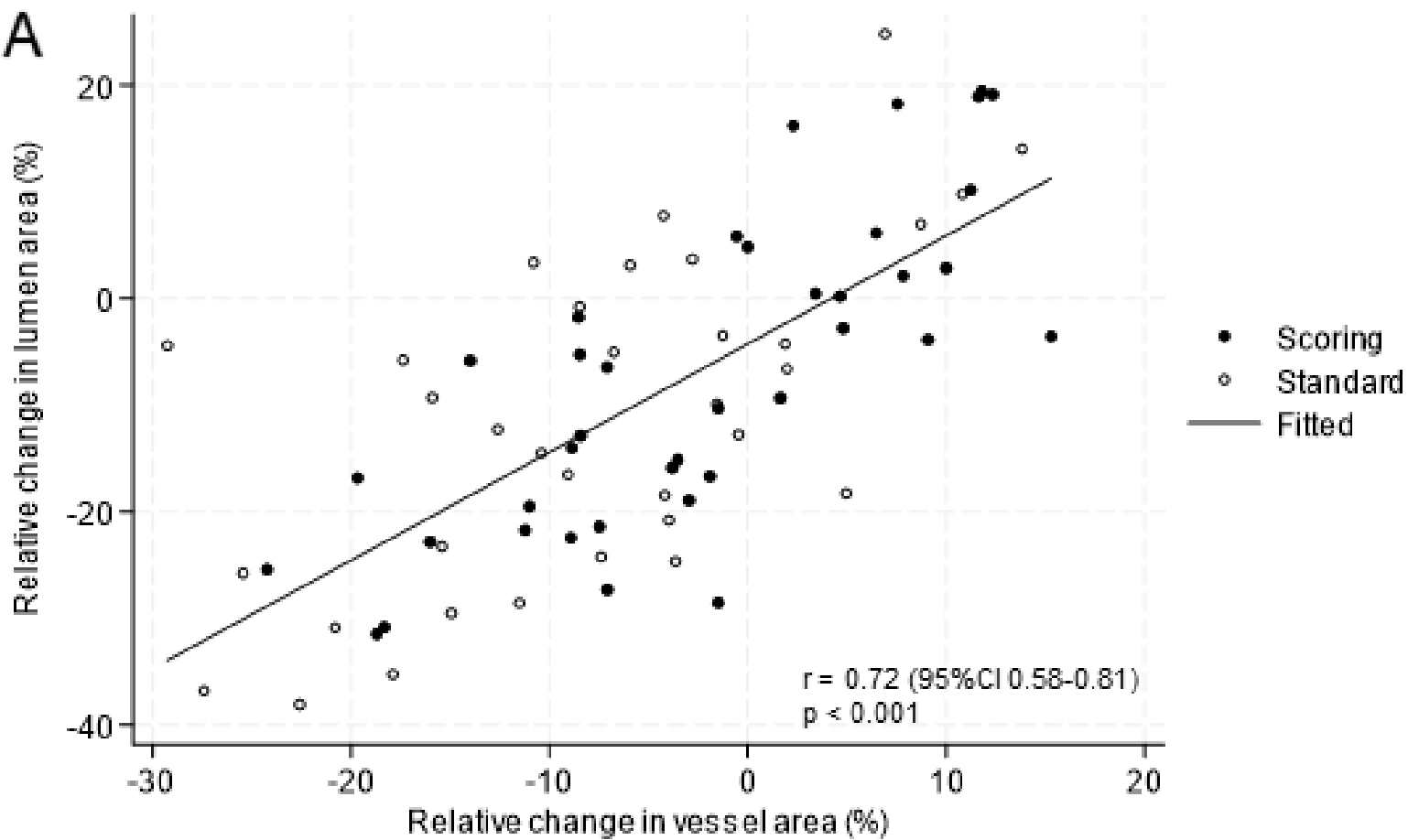
A. Correlation between relative change in lumen area (%) and relative change in vessel area (%) at the lesion site. B. Correlation between relative change in lumen area (%) and relative change in plaque area at the lesion site









**A****B**